

Magnetic anisotropy and relaxation behavior of six-coordinate tris(pivalato)-Co(II) and -Ni(II) complexes

Shu-Yang Chen,^a Hui-Hui Cui,^a Yi-Quan Zhang,^{b*} Zhenxing Wang,^{c*} Zhong-Wen

Ouyang,^c Lei Chen,^d Xue-Tai Chen,^{a*} Hong Yan,^a Zi-Ling Xue^e

^a*State Key Laboratory of Coordination Chemistry, School of Chemistry and Chemical Engineering, Nanjing University, Nanjing 210023, China. E-mail: xtchen@nju.edu.cn.*

^b*Jiangsu Key Laboratory for NSLSCS, School of Physical Science and Technology, Nanjing Normal University, Nanjing 210023, China*

^c*Wuhan National High Magnetic Field Center & School of Physics, Huazhong University of Science and Technology, Wuhan 430074, China*

^d*School of Environmental and Chemical Engineering, Jiangsu University of Science and Technology, Zhenjiang 212003, P. R. China*

^e*Department of Chemistry, University of Tennessee, Knoxville, Tennessee 37996, USA.*

Electronic Supplementary Information

Preparations of **1** and **2**

Complexes **1** and **2** were prepared according to the reported procedures.^{S1,S2}

(NBu₄)[CoPiv₃] (**1**). Yield 34%. Anal. Calc. (found) for C₃₁H₆₃CoNO₆: C, 61.57; H, 10.50; N, 2.32. Found: C, 61.36; H, 10.51; N, 2.22%. IR (cm⁻¹): 2962 (s), 2875 (m), 1554 (s), 1485 (s), 1426 (s), 1377 (m), 1359 (m), 1227 (m), 1028 (w), 899 (m), 807 (w), 792 (w), 738 (w), 605 (m).

(NBu₄)[NiPiv₃] (**2**). Yield 36%. Anal. Calc. for C₃₁H₆₃NiNO₆: C, 61.59; H, 10.50; N, 2.32. Found: C, 62.58; H, 10.58; N, 2.32%. IR (cm⁻¹): 2962 (s), 2875 (m), 1540(s), 1485 (s), 1432 (s), 1360 (m), 1227 (m), 1028 (w), 901 (w), 793 (w), 738 (w), 668 (w), 607 (m).

Ab initio calculations

The XMS-CASPT2^{S3} in MOLCAS 8.2 program package^{S4} considering the effect of the dynamic electron correlation based on complete-active-space self-consistent field (CASSCF) method was performed on individual Co^{II} or Ni^{II} fragment (see Figure S3 for the calculated complete structure of complex **1**; see Figure S4 for that of complex **2**) on the basis of X-ray determined geometry of complexes **1** and **2**. For the first CASSCF calculation, the basis sets for all atoms are atomic natural orbitals from the MOLCAS ANO-RCC library: ANO-RCC-VTZP for Co^{II} or Ni^{II} ion; VTZ for close O; VDZ for distant atoms. The calculations employed the second order Douglas-Kroll-Hess Hamiltonian, where scalar relativistic contractions were taken into account in the basis set. After that, the effect of the dynamical electronic correlation was applied

using CASPT2. The spin-orbit couplings were then handled separately in the restricted active space state interaction (RASSI-SO) procedure. The active electrons in 10 active spaces considering the 3d-double shell effect (5+5') include all seven 3d electrons for Co^{II} and eight for Ni^{II}, and the mixed spin-free states are 50 and 25, respectively (all from 10 quadruplets and all from 40 doublets for Co^{II}; all from 10 triplets and all from 15 singlets for Ni^{II}). And then, Single_Aniso^{S5} program was used to obtain the \mathbf{g} tensors, energy levels, magnetic axes, *et al.*, based on the above XMS-CASPT2/RASSI calculations.

Table S1 Summary of crystal data for **1** and **2**

1		2	
Crystal system	Monoclinic	Crystal system	Monoclinic
Space group	$P2_1/c$	Space group	$P2_1/c$
Cell parameters	$a = 13.842(1)$ Å	Cell parameters	$a = 13.841(1)$ Å
	$b = 18.029(1)$ Å		$b = 18.532(1)$ Å
	$c = 14.790(1)$ Å		$c = 14.908(1)$ Å
	$\beta = 101.5(2)$ °		$\beta = 101.7(1)$ °
bond	bond lengths (Å)	bond	bond lengths (Å)
Co-O(1)	2.105(2)	Ni-O(1)	2.045(4)
Co-O(2)	2.147(2)	Ni-O(2)	2.084(4)
Co-O(3)	2.123(2)	Ni-O(3)	2.073(3)
Co-O(4)	2.145(2)	Ni-O(4)	2.092(3)
Co-O(5)	2.129(2)	Ni-O(5)	2.108(4)
Co-O(6)	2.123(2)	Ni-O(6)	2.067(4)
bond	bond angles (°)	bond	bond angles (°)
O(1)-Co-O(2)	62.18(8)	O(1)-Ni-O(2)	62.54(2)
O(3)-Co-O(4)	61.86(8)	O(3)-Ni-O(4)	61.48(1)
O(5)-Co-O(6)	62.00(8)	O(5)-Ni-O(6)	60.68(1)
O(1)-C(1)-O(2)	119.00(2)	O(1)-C(1)-O(2)	118.02(6)
O(3)-C(6)-O(4)	120.35(3)	O(3)-C(6)-O(4)	117.42(5)
O(5)-C(11)-O(6)	119.48(2)	O(5)-C(11)-O(6)	119.20(5)

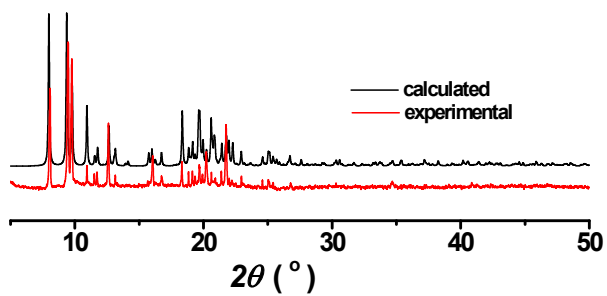


Figure S1 XRD patterns for complex **1**.

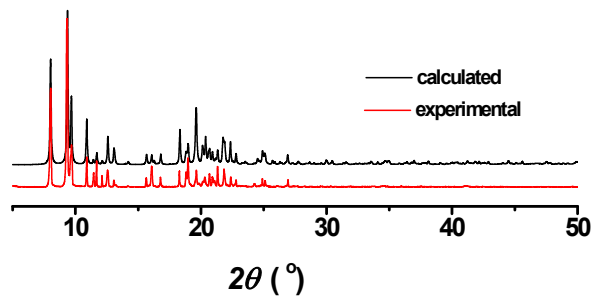


Figure S2 XRD patterns for complex **2**.

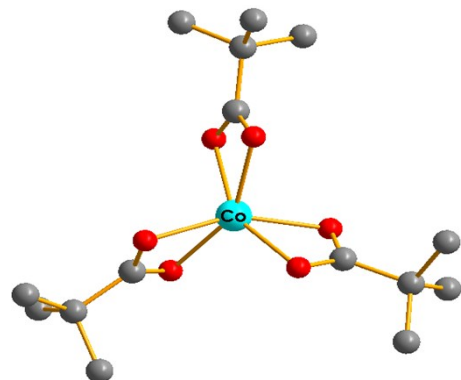


Figure S3 Calculated complete structure of **1**. H atoms are omitted for clarity.

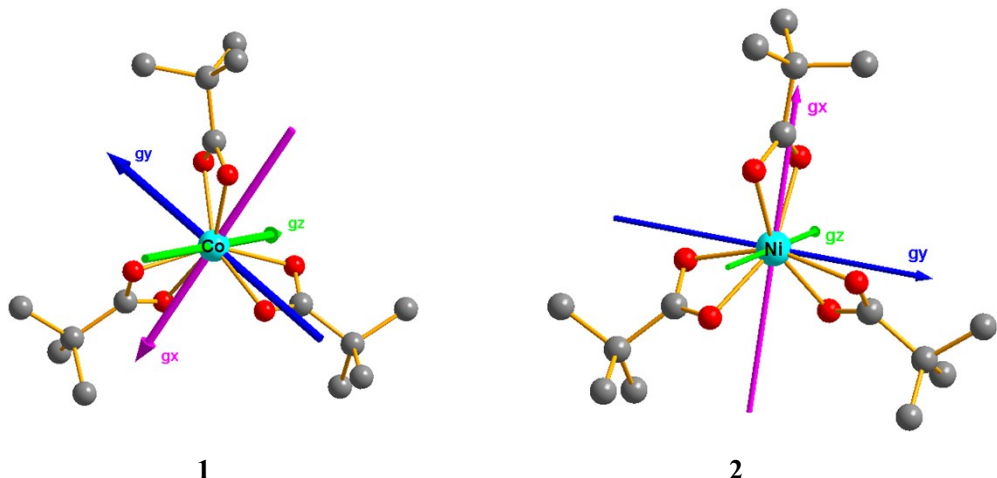


Figure S4 Orientations of the local magnetic axes of the ground doublet on Co^{II} or Ni^{II} ion of **1** and **2**.

Table S2 Calculated spin-free energies (cm⁻¹) of the lowest ten terms ($S = 3/2$) of the Co^{II} ion of complex **1**.

spin-free states	1
	E/cm^{-1}
1	0.0
2	447.1
3	1055.3
4	6415.4
5	6910.0
6	7233.7
7	13956.7
8	19909.2
9	20227.2
10	21019.3

Table S3 Calculated weights of the five most important spin-orbit-free states for the lowest two spin-orbit states of the Co^{II} ion of complex **1**.

Spin-orbit states	Energy (cm ⁻¹)	Spin-free states, Spin, Weights					
		1,1.5,0.7044	2,1.5,0.2203	3,1.5,0.0713	4,1.5,0.0014	5,1.5,0.0008	
1	0.0						
2	167.6	1,1.5,0.8875	2,1.5,0.0749	3,1.5,0.0299	5,1.5,0.0031	4,1.5,0.0022	

Table S4 Calculated energy levels (cm^{-1}), \mathbf{g} (g_x, g_y, g_z) tensors of the ground and first excited doublets of the Co^{II} of complex **1** using CASSCF with MOLCAS 8.2.

		1	
		E/cm^{-1}	\mathbf{g}
1	0.0	2.194	
		3.345	
		6.835	
2	167.6	1.329	
		1.733	
		5.428	

Table S5 Calculated zero-field splitting parameters D (E) (cm^{-1}) and \mathbf{g} (g_x, g_y, g_z) tensor of the lowest spin-orbit state on individual Ni^{II} fragment of complex **2** using XMS-CASPT2 with MOLCAS 8.2.

		2
$D(E)$	$-7.1\ (1.2)$	
\mathbf{g}	2.324	
	2.338	
	2.377	

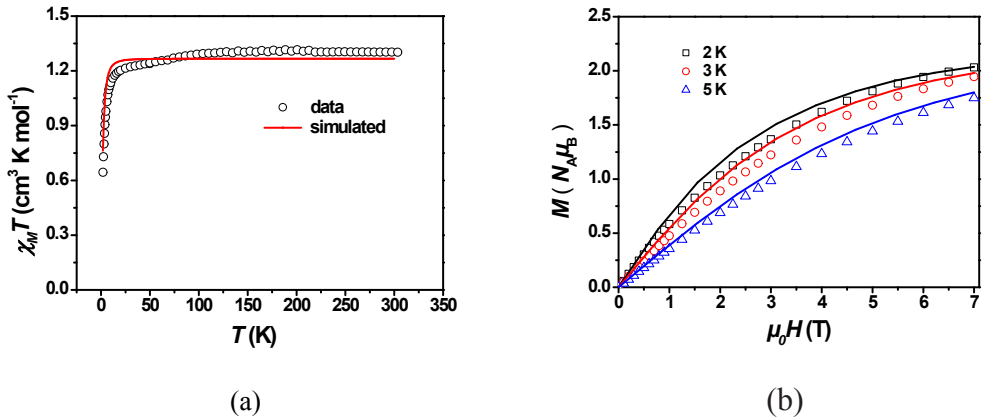


Figure S5 (a)The simulated curves of $X_M T-T$ and (b) $M-\mu_0 H$ generated by PHI

program using the Halmitonian parameters determined from HFEPR compared to the experimental curves of **2**.

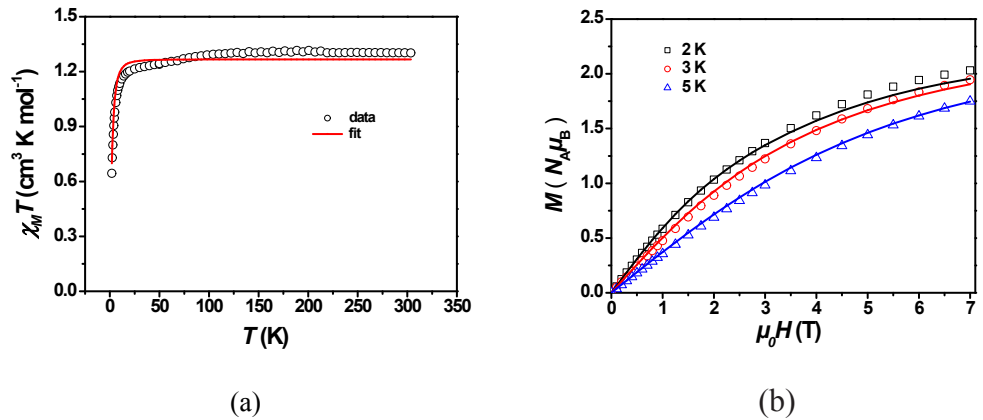


Figure S6 (a)Variable-temperature dc susceptibility data under an applied dc field of 0.1 T and (b) field dependent magnetizations for **2**. Solid lines are the fitting curves generated using spin Hamitonian by the *PHI* program with the g values fixed as those determined by HFEPR.

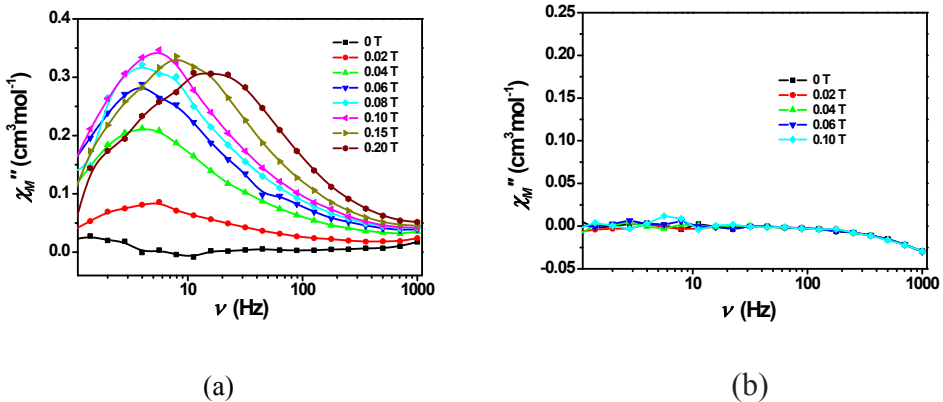


Figure S7 Frequency dependence of out-of-phase (χ_M'') ac susceptibility at 1.8 K

under the different applied static fields (from 0 to 0.2 T for **1**, (a); 0 to 0.1 T for **2**, (b)).

The solid lines are for eye guide.

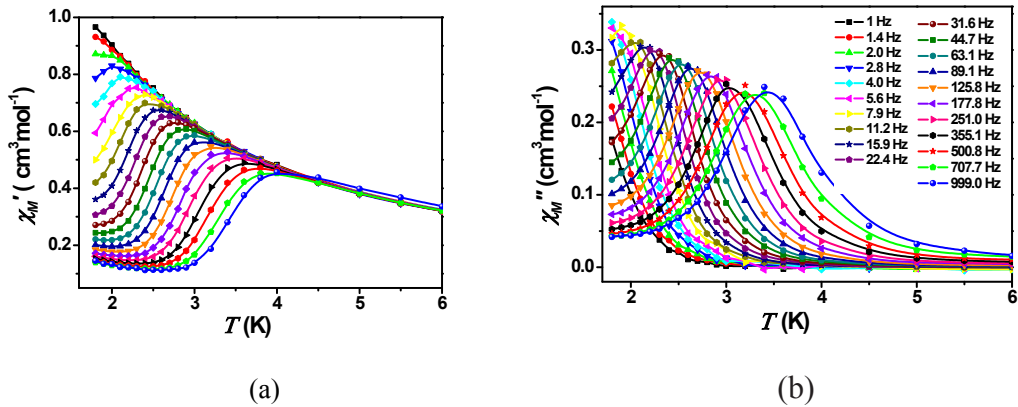


Figure S8 (a) Temperature dependence of in-of-phase (χ_M') and (b) out-of-phase ac susceptibility (χ_M'') at different ac frequency under a 0.1 T dc field for **1**. The solid lines are for eye guide.

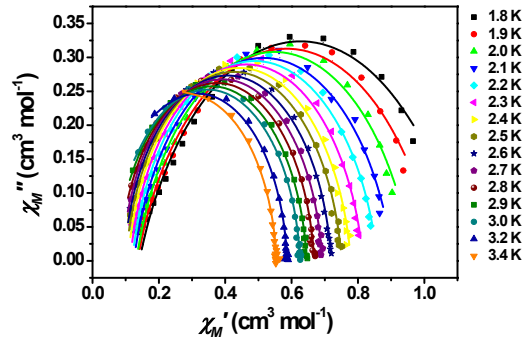


Figure S9 Cole-Cole plot obtained from the ac susceptibility data under 0.1 T dc field between 1.8 and 3.4 K for **1**. Solid lines represent the best fits to a generalized Debye model.

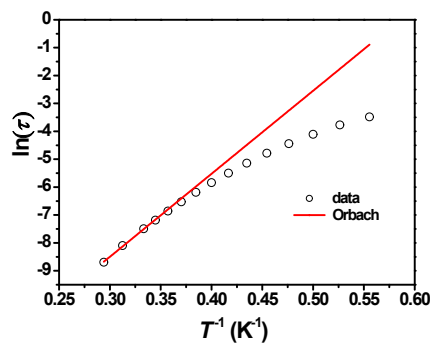


Figure S10 $\ln(\tau)$ vs T^{-1} plot of **1**. The red line presents the fitting to the linear relationship assuming that Orbach process is dominant in the high temperature range.

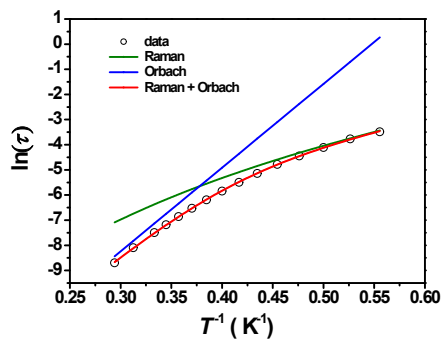


Figure S11 $\ln(\tau)$ vs T^{-1} plot of **1**. The red line represents a data fit to the Orbach and Raman processes simultaneously. The blue and green curves represent the contribution of Orbach and Raman process, respectively.

Table S6 The parameters obtained by fitting the Cole-Cole plot under 0.1 T for **1**

T(K)	χ_s	χ_T	τ	α
1.8	0.14	1.11	0.031	0.25
1.9	0.14	1.03	0.023	0.22
2.0	0.13	0.96	0.016	0.18
2.1	0.12	0.91	0.012	0.16
2.2	0.12	0.86	0.0084	0.14
2.3	0.11	0.82	0.0059	0.11
2.4	0.11	0.78	0.0041	0.097
2.5	0.10	0.75	0.0029	0.089
2.6	0.095	0.72	0.0020	0.076
2.7	0.090	0.69	0.0015	0.065
2.8	0.082	0.67	0.0010	0.060
2.9	0.075	0.65	0.00076	0.055
3.0	0.068	0.63	0.00056	0.053
3.2	0.048	0.59	0.00030	0.046
3.4	0.014	0.55	0.00017	0.052

Table S7 Dependence of the calculated energy levels (cm^{-1}), \mathbf{g} (g_x, g_y, g_z) tensors of the ground and first excited doublets of the Co^{II} of **1** with the angle φ from 0° to 60° using XMS-CASPT2 with MOLCAS 8.2. The angle φ of complex **1** is 28.71° .

	0°		10°		20°		28.71°	
	E/cm^{-1}	\mathbf{g}	E/cm^{-1}	\mathbf{g}	E/cm^{-1}	\mathbf{g}	E/cm^{-1}	\mathbf{g}
1	0.0	0.035	0.0	0.395	0.0	0.890	0.0	2.194
		0.036		0.406		1.016		3.345
		9.572		9.278		8.711		6.835
2	235.0	3.231	206.6	4.115	174.1	3.076	167.6	1.329
		3.256		3.903		3.532		1.733
		4.615		3.351		4.447		5.428
		40°	50°		60°			
	E/cm^{-1}	\mathbf{g}	E/cm^{-1}	\mathbf{g}	E/cm^{-1}	\mathbf{g}		
1	0.0	5.582	0.0	6.168	0.0	6.772		
		4.863		4.808		4.779		
		2.142		2.035		1.810		
2	136.1	0.269	166.7	0.600	183.0	0.914		
		0.368		0.648		0.967		
		5.904		5.608		5.161		

Table S8 Dependence of the calculated zero-field splitting parameters D (E) (cm^{-1}) and \mathbf{g} (g_x , g_y , g_z) tensor of the lowest spin-orbit state on individual Ni^{II} fragment of **2** with the angle φ from 0° to 60° using XMS-CASPT2 with MOLCAS 8.2. The angle φ of complex **2** is 28.08° .

	0°	10°	20°	28.08°
$D(E)$	124.3 (-2.7)	48.1 (-1.0)	13.6 (-0.5)	-7.1 (1.2)
\mathbf{g}	2.782	2.578	2.435	2.324
	2.750	2.567	2.428	2.338
	1.974	2.267	2.341	2.377
	40°	50°	60°	
$D(E)$	-14.9 (0.9)	-31.9 (1.2)	-42.7 (0.9)	
\mathbf{g}	2.282	2.262	2.245	
	2.295	2.273	2.258	
	2.394	2.582	2.627	

References

- S1 E. Fursova, G. Romanenko, R. Sagdeev and V. Ovcharenko, *Polyhedron*, 2014, **81**, 27.
- S2 E. Fursova, G. Romanenko and V. Ovcharenko, *Polyhedron*, 2013, **62**, 274.
- S3 (a) A. A. Granovsky, *J. Chem. Phys.*, 2011, **134**, 214113; (b) T. Shiozaki, W. Gyorffy, P. Celani and H.-J. Werner, *J. Chem. Phys.*, 2011, **135**, 081106; (c) L. Ungur and L. F. Chibotaru, *Chem. Eur. J.*, 2017, **23**, 3708.
- S4 (a) F. Aquilante, L. De Vico, N. Ferré, G. Ghigo, P.-Å. Malmqvist, P. Neogrády, T. B. Pedersen, M. Pitonak, M. Reiher, B. O. Roos, L. Serrano-Andrés, M. Urban, V. Veryazov and R. Lindh, *J. Comput. Chem.*, 2010, **31**, 224; (b) V. Veryazov, P. -O. Widmark, L. Serrano-Andres, R. Lindh and B. O. Roos, *Int. J. Quantum Chem.*, 2004, **100**, 626; (c) G. Karlström, R. Lindh, P.-Å. Malmqvist, B. O. Roos, U. Ryde, V. Veryazov, P.-O. Widmark, M. Cossi, B. Schimmelpfennig, P. Neogrády and L. Seijo, *Comput. Mater. Sci.*, 2003, **28**, 222.
- S5 (a) L. F. Chibotaru, L. Ungur and A. Soncini, *Angew. Chem. Int. Ed.*, 2008, **47**, 4126; (b) L. Ungur, W. Van den Heuvel and L. F. Chibotaru, *New J. Chem.*, 2009, **33**, 1224; (c) L. F. Chibotaru, L. Ungur, C. Aronica, H. Elmoll, G. Pilet and D. Luneau, *J. Am. Chem. Soc.*, 2008, **130**, 12445.